



UNIVERSITÀ POLITECNICA DELLE MARCHE
Repository ISTITUZIONALE

Self-oriented anisotropic structure of G-hydrogels as a delicate balance between attractive and repulsive forces

This is the peer reviewed version of the following article:

Original

Self-oriented anisotropic structure of G-hydrogels as a delicate balance between attractive and repulsive forces / Pepe, Alessia; Moretti, Paolo; Sakamoto Yoneda, Juliana; Carducci, Federica; Itri, Rosangela; Mariani, Paolo. - In: NANOSCALE. - ISSN 2040-3364. - ELETTRONICO. - 15:37(2023), pp. 15196-15205. [10.1039/d3nr01348k]

Availability:

This version is available at: 11566/320652 since: 2024-02-02T10:25:27Z

Publisher:

Published

DOI:10.1039/d3nr01348k

Terms of use:

The terms and conditions for the reuse of this version of the manuscript are specified in the publishing policy. The use of copyrighted works requires the consent of the rights' holder (author or publisher). Works made available under a Creative Commons license or a Publisher's custom-made license can be used according to the terms and conditions contained therein. See editor's website for further information and terms and conditions.

This item was downloaded from IRIS Università Politecnica delle Marche (<https://iris.univpm.it>). When citing, please refer to the published version.

(Article begins on next page)

Cite this: DOI: 00.0000/xxxxxxxxxx

Self-oriented anisotropic structure of G-hydrogels as a delicate balance between attractive and repulsive forces

Alessia Pepe,^{*a} Paolo Moretti,^a Juliana S. Yoneda,^{b,c} Federica Carducci,^a Rosangela Itri^b and Paolo Mariani^{*a}Received Date
Accepted Date

DOI: 00.0000/xxxxxxxxxx

Guanine (G) hydrogels are very attractive materials made by the supramolecular organization of G-derivatives in water. In this paper, hydrogels composed by guanosine 5'-monophosphate (GMP) and guanosine (Gua), that make long, flexible and knotted G-quadruplexes, were investigated by Small- and Wide-angle X-ray Scattering (SAXS and WAXS) to comprehend the origin of the unique orientational properties. The SAXS intensity, analysed at a fixed scattering vector modulus Q as a function of the polar angle, allowed us to derive the Maier-Saupe orientation parameter m . The strong dependence of m on hydrogel composition and temperature demonstrated that the preferred orientation is controlled by the quadruplex surface charge and flexibility. Indeed, a possible correlation between the orientation parameter m and the quadruplex-to-quadruplex lateral interactions was explored. Results confirmed that the balance between attractive and repulsive interactions plays a main role in the orientational anisotropy: quadruplex clusters lose their orientational property when attractive interactions decrease. The key role of the number of negative charges-per-unit-length of the G-quadruplex filaments was confirmed by Atomic Force Microscopy (AFM) observations. Indeed, directionality histograms showed that in the presence of large amount of Gua, G-quadruplexes follow other preferential orientations than those related to the strong interactions with the K^+ pattern on the mica surface. The fact that lateral quadruplex-to-quadruplex interactions, even in the presence of external (opposing) forces, can tune the hydrogel alignment in a given preferred direction opens novel possibilities for scaffold/3D printing applications.

1 Introduction

Guanine (G)-quadruplexes are four-stranded supramolecular helical structures formed by G-rich single-stranded nucleic acid sequences.¹ In these structures, four guanines are hydrogen-bonded through the non-canonical Hoogsteen scheme and the resulting G-quartets are stacked on top of one another.² G-quadruplex formation and stability are strongly related to the presence of monovalent cations (such as Na^+ and K^+), which enhance the base-stacking interactions by locating into the central cavity of the G-quadruplex to coordinate the O_6 carbonyl oxygen atoms of eight molecules of guanine belonging to two superposed G-quartets.³

In spite of the absence of the sugar-phosphate axial backbone, even the guanosine 5'-monophosphate (GMP) in aqueous solution

self-assembles to form G-quadruplexes (see Figure 1)⁴. The process is spontaneous, already occurs at high dilution and requires the presence of the proper monovalent cations.

In-solution X-ray and neutron scattering experiments established the structural characteristics of the G-quadruplexes^{5,6}: they are made by G-quartets, stacked at a distance of 3.4 Å and rotated with respect to each other by an angle of about 30°. Other characteristics were demonstrated: *first*, G-quadruplexes are surprisingly stable; *second*, they show a concentration and temperature-dependent length; *third*, lateral quadruplex-to-quadruplex interactions, measured by osmotic stress experiments, show a hydration and electrostatic contributions, mainly active at short and long distances, respectively, and connected to the quadruplex pitch^{7,8}. As a consequence of these properties, a columnar liquid crystalline lyotropic polymorphism occurs in water, with the formation of a cholesteric and an hexagonal phase when the GMP concentration increases.

Recently, the formation of G-quadruplexes over a large concentration and temperature range has been also demonstrated when adding guanosine (Gua) to GMP^{9,10}. Gua is electrically neutral but preserves the ability to form G-quartets: by modulating the

^a Department of Life and Environmental Sciences, Università Politecnica delle Marche, via Brecce Bianche, 60131 Ancona, Italy. E-mail: a.pepe@pm.univpm.it, p.mariani@univpm.it

^b Department of Applied Physics, Institute of Physics, University of Sao Paulo, Sao Paulo, Brazil.

^c Brazilian Synchrotron Light Laboratory (LNLS), Brazilian Center for Research in Energy and Materials (CNPEN), Campinas, Brazil.

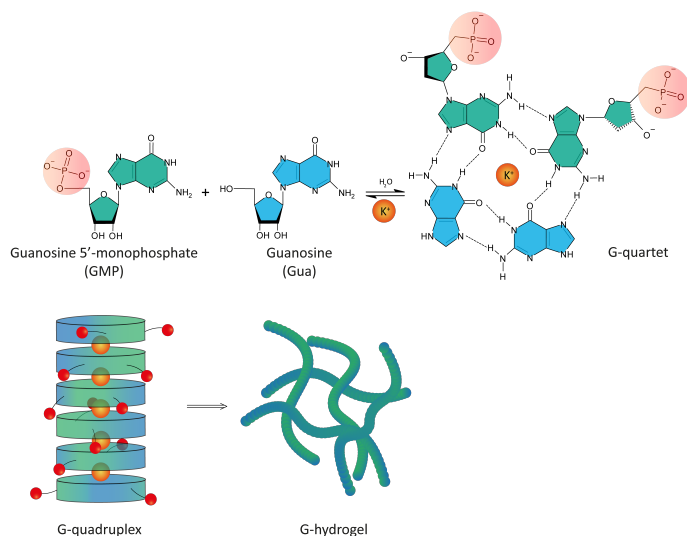


Fig. 1 Schematic representation of the self-assembling of guanosine 5'-monophosphate (GMP) and guanosine (Gua) in water solution. The first aggregation leads to the formation of the planar tetramers (G-quartets) that, in turn, organize in G-quadruplexes. Counter-ions (e.g. K⁺) are located in the inner cavity of the G-quartets, stabilizing the quadruplexes. Note that each GMP in the quartet results in a phosphate group on the external surface.

Gua/GMP molar ratio, e.g., by controlling the balance between electrostatic and van der Waals interactions among the quadruplexes, the formation of a transparent and stable 3D physical hydrogel has been demonstrated. AFM images and Small Angle X-ray Scattering (SAXS) confirmed the presence of G-quadruplexes but evidenced unusual properties, as the possibility to hydrate the gel up to a water volume fraction of 0.99 and the presence of an anisotropic order (already suggested by polarizing optical microscopy observation⁹).

Supramolecular materials obtained by self-assembly of low molecular weight biomolecules are extremely attractive for nanotechnology (from cell culture scaffolds to drug delivery) because of their very special properties, as self-assembling, tunability, self-healing, softness, external stimuli assembling/disassembling responsiveness, adaptability to environmental changes^{11–13}. Therefore, their structural characteristics merit to be deeply investigated. In this paper, X-ray scattering techniques have been used to describe the lateral interactions among the G-quadruplexes inside the gel and the strong alignment properties. In particular, flexibility, alignment and order parameters were studied as a function of Gua/GMP composition, temperature and dilution.

2 Materials and Methods

Guanosine 5'-monophosphate, sodium salt form (Santa Cruz Biotechnology, 99% purity), was converted into potassium salt by using acid-base titration, followed by drying and lyophilisation of the recovered solution. The lyophilised powder was redissolved in pure water, precipitated by adding three volumes of absolute ethanol and collected by centrifugation in a microcentrifuge tube at high speed (4000 rpm for 15 min). The pellet was resuspended in distilled water, at the concentration of 200 mg/mL. Guanosine (Sigma, St. Louis, USA; 99% purity) was suspended in water, at

the concentration of 150 mg/mL.

2.1 Hydrogel preparation

Hydrogels were prepared by mixing into a glass vial the precise volume of Gua and GMP solutions. The final water concentration was then reached by adding distilled water. The mixtures were heated up to 80°C (i.e. till the formation of a liquid transparent solution) and then left to cool down at room temperature. After 10 min equilibration at 20°C, the formed hydrogel resulted transparent and clear. The actual gel formation was confirmed by vial inversion tests, as previously reported⁹.

The final composition of the investigated Gua/GMP mixtures is indicated in Table 1. Note that Gua/GMP composition is indicated as molar ratio, while the water amount is reported as volume/volume percent (v/v %).

Table 1 G-hydrogel investigated conditions.

Gua/GMP molar ratio	v/v % water analysed at Diamond	v/v % water analysed at Sao Paulo
1 : 1	90, 98	85.0, 89.0, 93.0, 96.9, 97.3, 97.6, 98.1, 98.5, 98.6, 98.9, 99.1
1 : 2	90, 98	85.0, 89.0, 93.0, 96.9, 97.3, 97.7, 98.1, 98.5
1 : 4	90, 98	-

As Gua is poorly soluble in water, errors in adding Gua solution to the mixture were minimised by pipetting the stock solution several times before delivery. Errors on the Gua/GMP molar ratio not larger than 5% were estimated by gravimetric assay on delivery testing.

2.2 X-ray scattering experiments

Small angle and wide-angle X-ray scattering (SAXS and WAXS) experiments were performed at the I22 beamline of Diamond Light Source (Harwell, UK). The experiment exploited the mail-in service. The 3 m camera anisotropic SAXS/WAXS I22 setup and a Pilatus P3-2M (Silicon hybrid pixel detector, DECTRIS) detector with a pixel size of 172 μm² were used. The final investigated *Q*-range (*Q* being the modulus of the scattering vector, defined as $4\pi \sin \theta / \lambda$, where 2θ is the scattering angle) was 0.4 – 3.0 nm⁻¹ for SAXS and 3.0 – 50 nm⁻¹ for WAXS. Hydrogels were measured in 1 mm thin-walled capillary tubes.

SAXS experiments were also performed by using a NanoStar instrument (Bruker Corporation) at S. Paulo University (Brazil). The wavelength of the incident beam was $\lambda = 0.154$ nm and the explored *Q*-range extended from 0.5 to 4.0 nm⁻¹. Scattering data were recorded on a 2-dimensional Bruker CCD camera of 1024x1024 pixels. Experiments were performed as a function of the temperature, from 20 to 90 °C, with an heating rate of 1 °C min⁻¹. Hydrogels were measured in 1 mm sample holders provided with kapton windows.

SAXS (and WAXS) two-dimensional (2D) data were corrected for background, detector efficiency, and sample transmission and then analysed by using *ImageJ* macros. Further analyses were performed on *I(Q)* vs. *Q* curves obtained by radial average of the 2D data.

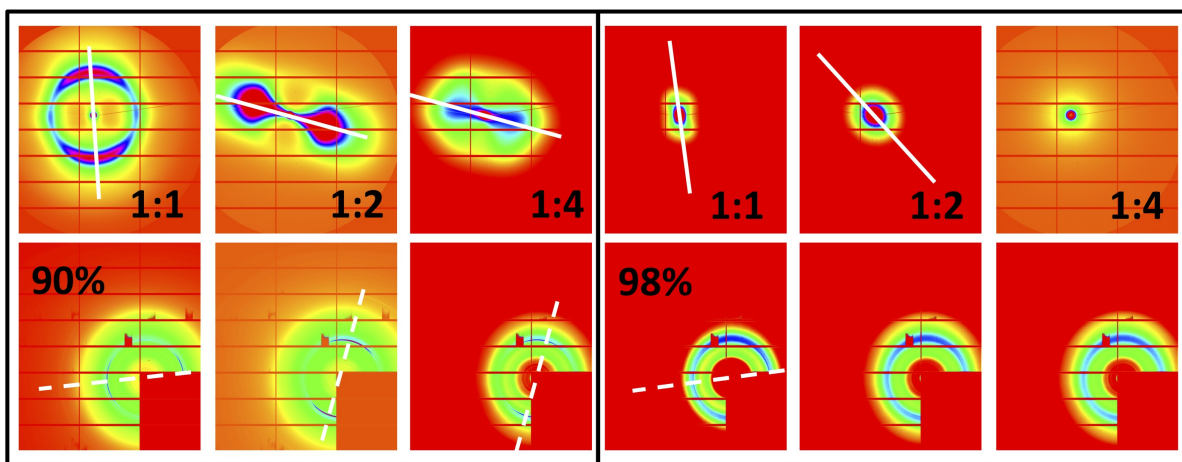


Fig. 2 2D SAXS results obtained at 90 (left box) and 98% of water (right box) from Gua/GMP hydrogels. White lines represent the main scattering orientations (solid line, equatorial scattering; dashed line, meridional scattering). See Fig. 3 for the experimental set-up.

2.3 Atomic force microscopy

AFM images were obtained by using an AIST-NTÖs Scanning Probe Microscopy (Horiba Scientific). Images were generated in non-contact mode with a pyramidal silicon tip with 8 nm radius. All images were acquired at room temperature with a resolution of 512x512 pixels and scan rate of 0.5 Hz to prevent sample deformations induced by the tip. Images were flattened using flatten background function of Gwyddion software¹⁴. Gua/GMP hydrogels prepared at different compositions were diluted up to 200-fold before dripping 5 μ l of the diluted solution onto a freshly cleaved mica surface. The solution on the mica was then dried by gentle blowing a stream of nitrogen.

AFM images were analysed by using *Fiji*, the open source image processing software. To derive the preferred orientation of structures present in the input image, the *Directionality* analysis macro 2.3.0 was used. The Fourier analysis method with a number of bins equal to 90 was used. The macro computes a directionality histogram, indicating the amount of structures in a given direction (for our intent, histograms are from -90° to 90°): as expected, images with isotropic content give a flat histogram, whereas a oriented-peak histogram results from images with structures preferentially oriented¹⁵.

3 Results and Discussion

3.1 Anisotropic scattering and order parameter determination

SAXS/WAXS experiments were first performed to confirm the G-hydrogel orientational properties already reported by Carducci et al.⁹. Figure 2 shows the 2D data obtained at Diamond for the 1:1, 1:2 and 1:4 Gua/GMP hydrogels prepared at two different water contents, namely 90 and 98% water.

The hydrogel orientational organization is fully confirmed by the fan-like profiles observed in the small-angle region (Fig. 2, upper row) and by the anisotropy of the wide-angle diffraction arcs (Fig. 2, lower row). The hydrogel orientational order is very evident at 90% of water, but it is also detected in two of the more diluted hydrogels, where anisotropic properties are ex-

pected to be absent. Two points are particularly relevant: first, a random orientation is observed, suggesting that orientational organisation does not depend on the sample holder (1 mm capillary, in this case); second, the oriented SAXS pattern, which provides information on the long-range (anisotropic) ordering of the G-quadruplexes in the hydrogels, distributes orthogonally to the WAXS arcs, which are related to the G-quartet stacking. According to the G-quadruplex structure (see Figure 1), such a result confirms that the observed X-ray scattering anisotropy depends on the preferential G-quadruplex parallel alignment in the hydrogel matrix.

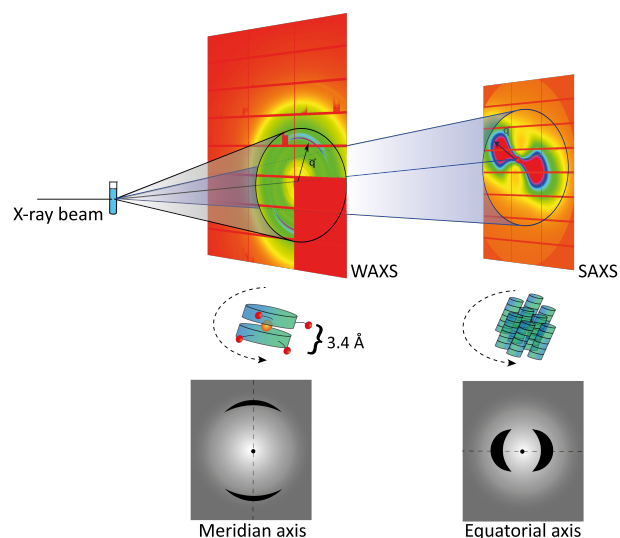


Fig. 3 Set-up for the SAXS/WAXS experiment and anisotropic scattering denominations. In liquid-crystal field, meridional scattering is associated to short-range order, while equatorial scattering is associated to long-range order¹⁶. The obtained WAXS and SAXS 2D patterns have been then rotated to orient them according to the meridional and equatorial directions, respectively: thus, the scattering along the meridional axis is related to the π - π stacking of G-quartets, while the scattering on the equatorial axis is associated to the lateral interactions among the G-quadruplexes.

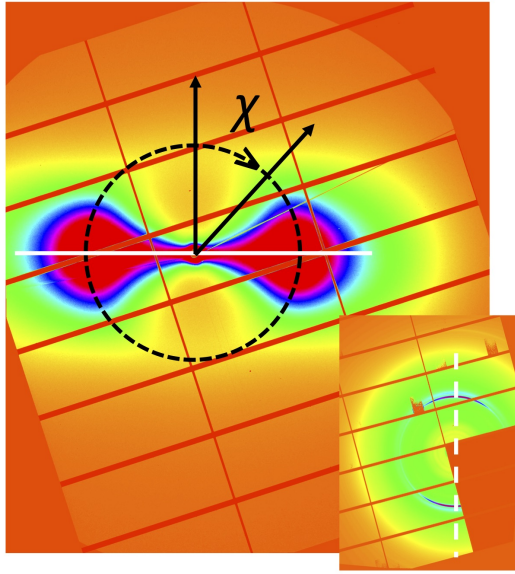


Fig. 4 SAXS and WAXS 2D profiles from 1:2 Gua/GMP hydrogel. Both images have been rotated by -17° . White lines represent the main scattering orientations (solid line, equatorial scattering; dashed line, meridional scattering). Black lines define the polar angle χ .

To discuss the oriented results, the terminology used for describing the anisotropic scattering from fibres and liquid crystal systems¹⁶ will be here employed (see the schematic diagram of an X-ray scattering experiment in Figure 3): the oriented SAXS pattern lies along the equatorial axis, while the WAXS arcs are centred along the meridian. This geometry is easily obtained by contemporaneous rotation of the 2D SAXS and WAXS related profiles. As a representative case, the 2D data for the 1:2 Gua/GMP sample at 90% water are presented in Figure 4 (compare with unrotated data in Figure 2) after rotation of -17° : SAXS spots are on the equatorial direction, while the WAXS pattern is on the meridian.

As suggested by the different shape of the oriented SAXS patterns in Figure 2, the G-quadruplex alignment in the hydrogel matrix depends on composition. Assuming that in the SAXS region the scattering is only due to the lateral interferences between quadruplexes¹⁷, a direct information on the degree of ordering of these particles can be obtained by analysing such intensity as a function of the polar angle χ , as defined in Figure 4. The χ -dependence of the integrated X-ray intensity profile in the SAXS region can be in fact related to the Maier-Saupe orientational distribution function $f(\beta)$ ^{18,19} of the clusters of G-quadruplexes in the ordered structure (β is the angle existing between the principal axis of a quadruplex and the average orientation of all the principal quadruplex axes, e.g., the *director* direction in columnar liquid crystal terminology)¹⁹:

$$f(\beta) = \frac{1}{Z} \exp(m \cos^2 \beta) \quad (1)$$

where m is a (positive) parameter related to the width of the

distribution and Z is a normalization factor given by:

$$Z = 4\pi \frac{\exp(m)}{\sqrt{m}} D(\sqrt{m}) \quad (2)$$

where D is Dawson's integral. Note that at larger m values, the distribution is narrower, meaning that the quadruplexes are more likely to be oriented in a narrow range around $\beta=0$.

According to Mills et al.¹⁹, m can be obtained by analysing the $I(\chi)$ scattering data according to the following equation:

$$I(\chi) = I_b + \frac{C\sqrt{m}}{8\exp(m) D(\sqrt{m})} \exp\left(\frac{m\cos^2 \chi}{2}\right) I_0\left(\frac{m\cos^2 \chi}{2}\right) \quad (3)$$

where I_b is the constant background, I_0 is a modified Bessel function of the first kind and C can be adjusted to take into account different amounts of sample or different exposure times.

A few examples of experimental $I(\chi)$ data, integrated in the Q -range between 0.7 and 0.8 nm^{-1} , are shown in Figure 5, along

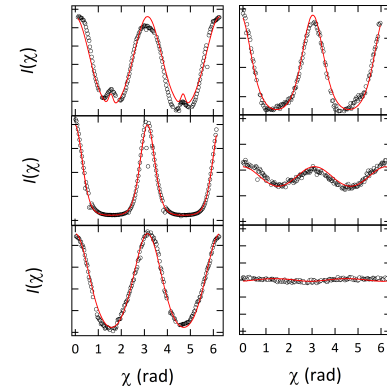


Fig. 5 Polar angle dependence of the scattering intensity, $I(\chi)$, measured at the same Q (between 0.7 and 0.8 nm^{-1}) from different hydrogels. Top, middle and bottom rows refer to 1:1, 1:2 and 1:4 Gua/GMP hydrogels. Left and right graphs concern hydrogels prepared at 90 and 98% water, respectively.

with fitting results obtained by using Equation 3. Table 2 reports the derived orientation parameters m .

Table 2 Orientation m parameters obtained by fitting the Eq. 3 to the experimental $I(\chi)$ data (see Fig. 5).

Gua/GMP	90% water	98% water
1:1	3.0	1.9
1:2	6.2	1.6
1:4	1.4	0.3

Equation 1 has been then used to calculate $f(\beta)$ for all the analysed conditions. The results in term of the Maier-Saupe orientational distribution function and of the function $f(\beta)\sin\beta$, which is proportional to the fraction of rods oriented at the angle β , are reported in Figure 6.

According to the SAXS profiles, it is interesting to observe that G-hydrogel dilution causes a reduction in the intensity of the $f(\beta)$ distribution function and an increase in its width, e.g. a contemporaneous decrease and enlargement of the probability function

$f(\beta)\sin\beta$. It can be also noticed that in the 1:1 hydrogel, the $I(\chi)$ scattering at 90% water can be deconvoluted into scattering from two separate and orthogonal quadruplex distributions, with different order parameters (see the second fitting line in Figure 5). On the contrary, at 98% water, only one distribution exists. This difference will be confirmed below.

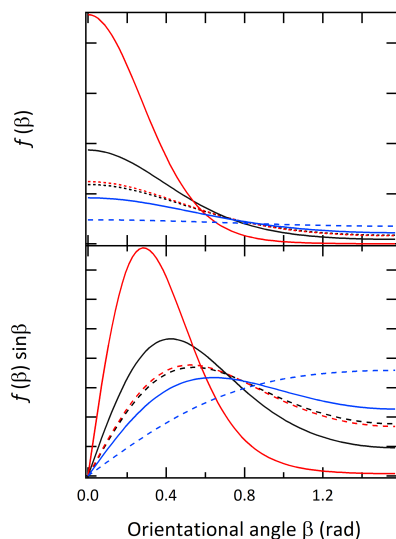


Fig. 6 Maier-Saupe orientational distribution functions, $f(\beta)$ and $f(\beta)\sin\beta$ (top and bottom graph, respectively). Solid and dashed lines concern hydrogels prepared at 90 and 98% of water, while colours refer to 1:1 (black), 1:2 (red) and 1:4 (blue) Gua/GMP hydrogels.

Further, SAXS experiments on 1:1 and 1:2 Gua/GMP hydrogels were also performed as a function of temperature (up to 90°C) and water composition (up to 99%). 2D scattering results, reported in Figure 7, show not only that orientational properties maintain on heating and on strongly diluted conditions, but also that the double distribution of G-quadruplex clusters is a peculiar characteristic of 1:1 hydrogels at low hydration. Indeed, as shown in Figure 7, the 2D scattering profiles observed from 85 to 93%, at least at low temperature, are similar to the one shown in Figure 2.

The 2D scattering profiles were then analysed as described. The m dependence on temperature and water compositions is shown for the different hydrogels in Figure 8: errors are quite large, but data show that both dilution and temperature increase destroy the quadruplex orientation. Moreover, 1:2 Gua/GMP hydrogels show strong orientational properties, but the order parameter quickly reduces as far as water concentration increases; on the contrary, the width of the distribution in 1:1 Gua/GMP samples is larger, but more stable against dilution.

It is then evident that the orientational properties, but also their dependence on temperature and concentration, are modulated by hydrogel composition, which in turn controls the G-quadruplex interactions and stability. In other words, a strong orientational anisotropy is expected when the amount of GMP in the hydrogel is low because of the consequent reduction of lateral quadruplex-to-quadruplex electrostatic repulsive interactions, which makes nearly parallel orientation of the quadruplexes possible. Accord-

ingly, the orientation parameter m in Table 2 increases in going from 1:4 to 1:1 at 98% water. However, Gua-rich filaments are very flexible and adhesive (because of the reduction in charge density and the increase of hydrophobicity), so that the correlation between Gua/GMP ratio and orientational anisotropy is certainly not linear (see the m values obtained at 90% water in Table 2). Moreover, interaction effects and flexibility/adhesiveness combine with G-quadruplex stability: as suggested by Figure 8, 1:1 hydrogel shows a lower orientational anisotropy but quadruplexes are very stable on dilution; on the contrary, 1:2 hydrogel shows a higher orientational anisotropy but on dilution quadruplexes shorten and begin to dissolve. In conclusion, a general trend for the dependence of the orientational parameter m on the hydrogel composition cannot be easily derived.

3.2 Interaction analysis

$I(Q)$ vs. Q curves were obtained by radial average of the 2D scattering images. Representative results are shown in Figs 9 (as a function of hydrogel composition) and 10 (as a function of temperature). Concerning the WAXS profiles, no changes were detected with composition, other than a minor visibility of the the 3.4 Å peak at larger water content. This fact is very relevant, as the observation of the 3.4 Å peak confirms the presence of G-quadruplexes at all the investigated conditions.

On the contrary, the SAXS scattering profiles depend on hydrogel composition (Fig. 9). No special SAXS features were in fact observed in hydrogels at 98% of water, while a narrow band, centred at about 0.1 Å^{-1} , is detected in samples at 90% water. However, as far as the GMP content in the hydrogels increases (e.g., from 1:1 to 1:4), the narrow band moves to lower Q , while its intensity decreases: as the quadruplex charge-per-unit-length increases with the GMP content, such a behaviour is indicative of an increased contribution of the electrostatic repulsion on the lateral interactions among the quadruplexes. Temperature has similar effects (shift of the band position to lower Q and decrease of its intensity), but the origin is clearly different: by heating, the larger quadruplex thermal fluctuations and undulations induce an increase of the repulsive lateral forces and consequently a higher quadruplex-to-quadruplex separation and a larger hydrogel disorder.

Direct information on structural and interaction properties can be retrieved by using simple model to fit to the SAXS data: at larger dilutions (as at 98% water), curves were analysed by using the mass fractal Teixeira model, which considers flexible cylinders as building blocks²⁰, while at lower dilutions (e.g., below 95% water), curves were analysed considering a hard sphere plus square well potential model for cylindrical objects²¹. In particular, the square-well potential (of width σ and depth U_0 , in which positive values correspond to an attractive potential well) was observed to be adequate to obtain a good fit to the experimental data

The obtained fitting curves are superimposed to scattering profile in Figs 9 and 10, while the most relevant fitting parameters are shown in Table 3.

Concerning the more diluted systems, the SAXS fitted param-

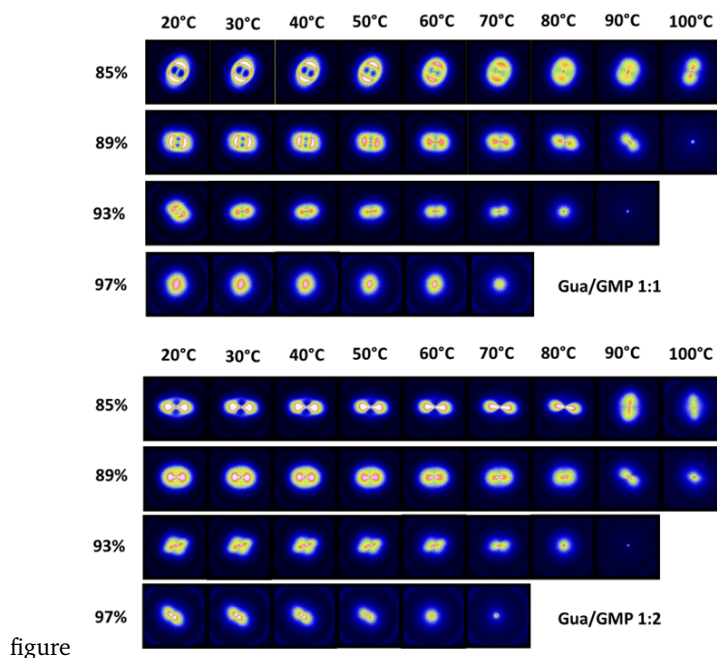


Fig. 7 2D SAXS results obtained as a function of composition and temperature from 1:1 and 1:2 Gua/GMP hydrogels. Water concentrations (rows) and temperatures (columns) are indicated in the figure.

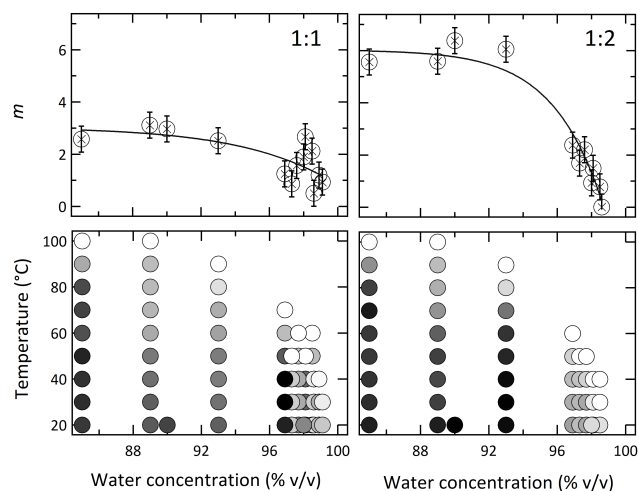


Fig. 8 Dependence of the orientation parameter m on water composition and temperature. Upper graphs show the dilution effects for the 1:1 and 1:2 Gua/GMP hydrogel at 20° (left and right side, respectively). Lower graphs are concentration/temperature diagrams (left side, 1:1; right side, 1:2 Gua/GMP hydrogels) showing the orientation parameter m in grayscale, from black, $m = 6$, to white, $m < 0.1$.

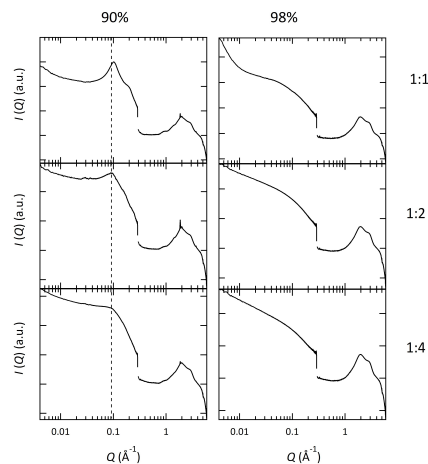


Fig. 9 SAXS and WAXS 1D curves obtained at different Gua/GMP and water compositions, as indicated. The dashed line is a eye guide to better follow the change in position of the narrow band observed in hydrogels prepared at 90% water.

eters confirm a fractal regime in between 1 and 5/3, suggesting that the hydrogel quadruplexes behave like a polymer with semi-flexible chains. Moreover, the fitted Kuhn length indicates that quadruplex flexibility decreases moving from 1:1 to 1:4 quadruplexes. It is obvious that a significant part of quadruplex rigidity is due to charge repulsions between GMP phosphates stacked along the helix: the replacement of GMP with Gua reduces the number of charges-per-unit-length then increasing the flexibility (note that asymmetric neutralisation of phosphates should even-

tually induce a substantial quadruplex bending).

Parameters obtained by the model fitting to the SAXS data related to the more concentrated hydrogels confirm that the lateral attractive interactions decrease with temperature and compositions (both by increasing the GMP content in the quadruplexes and by diluting the hydrogel). As discussed above, such a behaviour is due to the increased contribution of the Coulomb repulsion to the lateral forces (due to the increased GMP / Gua molar ratio) and/or to the increased repulsive steric forces associated to enhanced quadruplex thermal fluctuations and undulations (see also⁹).

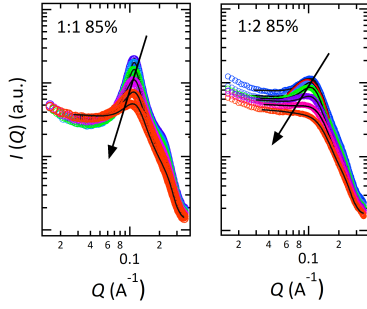


Fig. 10 SAXS 1D curves obtained from 1:1 and 1:2 85% water hydrogels at different temperatures (from 20 to 70°C, with 10° of interval), as indicated by a rainbow 6 colors scheme (from blu to red). Curves have been fitted by a hard sphere plus square well potential model.

Table 3 Fitted parameters for the 1:1 hydrogels at 89 and 85% of water at different temperatures; the 1:2 hydrogel at 89% of water and at different temperatures; 1:1, 1:2 and 1:4 hydrogels at 98% water.

1:1, 85%	20°C	30°C	40°C	50°C	60°C	70°C	80°C
R (Å)	9.9	10.0	10.1	10.4	10.6	10.7	10.6
h (Å)	104.7	104.2	102.5	98.6	93.5	90.6	88.7
U_0 (kT)	7.7	7.6	6.7	5.4	3.8	2.5	1.4
σ (Å)	3.8	3.8	4.4	4.8	5.1	4.7	5.7
1:1, 89%	20°C	30°C	40°C	50°C	60°C	70°C	80°C
R (Å)	10.5	10.5	10.6	10.8	10.8	10.8	10.7
h (Å)	138	138	133	127	119	115	105
U_0 (kT)	5.6	5.0	4.1	2.5	1.6	0.4	-
σ (Å)	3.2	4.6	4.2	5.2	5.0	4.5	-
1:2, 89%	20°C	30°C	40°C	50°C	60°C	70°C	80°C
R (Å)	11.3	11.4	11.3	11.2	11.0	-	-
h (Å)	108	109	110	108	108	-	-
U_0 (kT)	1.88	1.00	0.93	0.37	-	-	-
σ (Å)	10.8	10.7	9.9	10.8	-	-	-
98%, 20°C	1:1	1:2	1:4				
fractal dimension	1.46	1.14	1.15				
correlation length, d (Å)	27.5	80.6	113.9				
Kuhn Length, b (Å)	4.6	5.4	8.0				
Contour Length, L (Å)	143.9	119.3	116.3				
R (Å)	8.9	9.9	7.9				
Length polydisp	0.0024	0.0023	0.0023				

The origin of the attractive contribution to the lateral forces can be discussed. By osmotic stress method, we measured the force between GMP quadruplexes in KCl solutions^{7,8}. Two contributions were recognised: the first one was electrostatic, effective at large distances and strongly dependent on salt concentration; the second was hydrational, dominating at interaxial separations smaller than about 3 nm and rising steeply as the quadruplexes approach each other, preventing the coalescence of the helices. The addition of the electrically neutral G, which substitutes a number of GMP molecules along the quadruplexes, determines an overall charge reduction (as well as a change in the helix-specific charge distribution), but also the appearance of attractive forces between quadruplex regions rich in Gua¹⁰. These attractive forces are of Van der Waals or hydrophobic origin and are responsible for the hydrogel formation, as they contribute to the establishment of the distance of closest contact for the aggregates, and allow other interactions to take over for gel stability.

3.3 Orientational anisotropy versus G-quadruplex interactions

It is evident that the delicate and precise balance between attractive and repulsive lateral interactions between quadruplexes account for the stability of the G-hydrogels, but should also play an important role on the observed orientational anisotropy. Noteworthy, a possible correlation between the hydrogel local ordering properties and G-quadruplex interaction parameters was then considered by plotting the width and depth of the attractive square-well potential ($\sigma()$ and $U_0(kT)$, respectively) as a function of the orientation parameter m (see Fig.11). Because data are quite noisy, only two GMP/Gua compositions, at three different dilutions and temperatures, were considered.

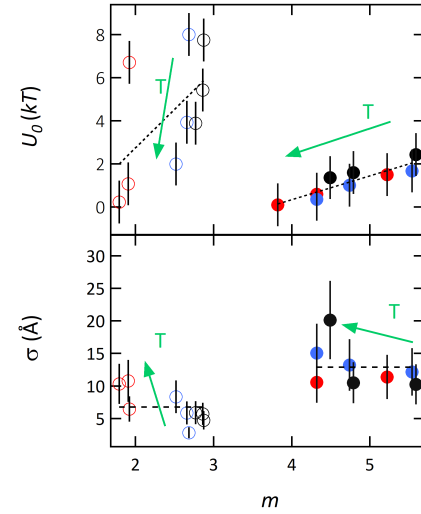


Fig. 11 Correlation between the G-quadruplex interaction potential and the orientation parameter m at different compositions (open and filled symbols refer to 1:1 and 1:2 hydrogel, respectively) and dilutions (black, blue and red symbols are for 85%, 89% and 93% of water, respectively)

A perusal of the data clearly shows that there is a clear correlation between the well depth and m , regardless the Gua/GMP composition and hydrogel temperature. On the other end, the potential width σ is nearly constant over m . It can be deduced that the well depth reduction induced both by temperature (see the arrows) and dilution (see the symbol colours) scales to lower m , meaning that quadruplexes lose their orientation when the attractive interactions decrease.

Noticeable is the fact that the well depth reduction rate for 1:1 hydrogel is 3 times larger than for 1:2 hydrogel (3.6 kT/ m than 1.1 kT/ m): therefore, interactions among 1:1 quadruplexes are rather strong but very sensitive to temperature changes. Probably, the increased flexibility due to the attenuated charges-per-unit-length in 1:1 quadruplexes exerts a strong impact on the balance between attractive and repulsive lateral forces. Orientational properties are however different in 1:1 and 1:2 hydrogels. The 1:2 quadruplexes orient in narrow angular range (larger m) with respect to the 1:1 quadruplexes. Probably the attractive contributions in 1:1 hydrogels are very high: the G-quadruplex stickiness induces non-specific aggregation which manifests in a broad alignment around the director direction. On the contrary, in the

1:2 hydrogels the repulsive contribution guarantees an ideal interaction potential which reflects in a very narrow, and stable, orientational distribution function of the G-quadruplexes.

3.4 Preferred orientation of G-quadruplex in AFM images

AFM images confirm the presence of the 3D net for all the different analysed hydrogels (see Fig. 12). In particular, an interconnected network of flexible quadruplexes is detected, and the presence of double and multiple-braided quadruplexes as well as of knots appear well documented¹⁰. However, the analysis with the *Directionality* macro showed that quadruplexes follow some preferential directions with respect to the support surface: direction-

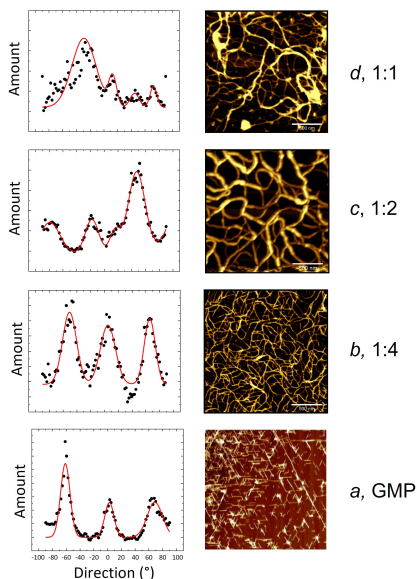


Fig. 12 AFM results: right side, AFM images obtained from the investigated system; left side, directionality histograms. From the top: 1:1, 1:2 and 1:4 G-hydrogels; GMP solution (200 mg/ml).

ality histograms show in fact a number of peaks, whose position and width depend on G-hydrogel composition. It should be mentioned that AFM samples are dripped on a mica surface, so that some directionality is certainly dependent on the interactions between the fine ultrastructure of the mica support and the surface of the charged G-quadruplexes, as already reported^{22,23}. Indeed, mica is a phyllosilicate mineral composed by a TOT-c structure, e.g., TOT sheets made by an octahedrally coordinated aluminium atom layer (O-layer) sandwiched between two identical layers of silicon-oxygen tetrahedra (T-layers) and bonded to each other by potassium cations (c). After cleavage, the mica surface reveals a regular, quasi-hexagonal array of oxygen atoms with a K^+ ion inside each hexagon (the quasi-hexagonal unit cell parameters are $a=0.52$ nm and $b=0.9$ nm²³). As the K^+ pattern matches very well the repeat distance of the negatively-charged phosphate groups of GMP on the quadruplexes, they will line up along the three possible directions of vector **a**, which result correlated of an angle of 60°.

This is evident in samples where G-quadruplexes are made by GMP only²³. Because the high number of phosphate groups

on the surface, the AFM image (Fig. 12, **a, GMP**) shows G-quadruplexes perfectly aligned on the mica surface along the three preferential directions: accordingly, three narrow peaks, correlated by 60°, characterise the directionality histogram (see Tab. 4). A very similar situation is observed also for the 1:4 hydrogel (see the Fig. 12, **b, 1:4**). The peaks in the directionality histogram are still narrow, equally populated and correlated by 60°. On the contrary, when the GMP content decreases, hydrogels appear less affected by the mica surface. Indeed, Figs 12 **c, 1:2** and **d, 1:1** show a more complex G-quadruplex alignment: the 4 peaks which are observed in the directionality histogram for the 1:1 and the 1:2 hydrogels are only in part correlated with the K^+ pattern (see Table 4, which reports the derived orientation parameters) indicating that other mechanisms modulate the alignment of the G-quadruplexes. According to the SAXS/WAXS results, it can be suggested that in low-charged hydrogels, the quadruplex-to-quadruplex lateral interactions exceed the effect of the K^+ pattern on mica surface and keep the G-quadruplexes preferentially oriented in other directions. In Tab. 4 are summarised the preferential directions for all the analysed cases.

Table 4 Position and width (in angular degrees) of the peaks observed in the directionality histograms as obtained by the *Fiji* plugin *Directionality*. The parameters of the peaks uncorrelated to others are in bold.

Sample	1st Peak	2nd Peak	3th Peak	4th Peak
1:1	-29.0, 35.0	13.0, 11.5	45.0, 13.0	72.4, 10.0
1:2	-79.0, 29.0	-17.8, 19.5	15.8, 15.5	47.0, 24.6
1:4	-50.9, 20.4	4.8, 21.9	65.6, 16.0	-
GMP	-59.3, 13.6	2.6, 13.4	68.5, 22.2	-

It should be observed that such self-driven anisotropy will be further analysed by AFM by using other substrates, that can avoid or at least reduce the electrostatic interactions with G-quadruplexes or after freeze-drying the hydrogels, so that the eventual nanofiber alignment will not be contaminated by the substrates.

4 Conclusions

X-ray scattering and AFM techniques have been used to assess the orientational properties of G-quadruplex clusters in G-hydrogels. From SAXS 2D profiles, the Maier-Saupe orientation parameter m has been derived. The observed dependence on composition and temperature suggests that preferred orientations is controlled by the Gua/GMP ratio, which in turn imposes the quadruplex surface charge and flexibility. The fitting of the SAXS 1D profiles to derive the quadruplex-to-quadruplex lateral interactions confirmed that the balance between attractive and repulsive interactions plays a central role in orientational anisotropy: quadruplex clusters lose their unique preferred orientations when attractive interactions decrease, for example by increasing temperature or by hydrogel dilution.

Directionality histograms derived from AFM images of G-hydrogels prepared at different composition confirmed the key role of the charges-per-unit-length in the G-quadruplexes. Indeed, histograms showed that G-quadruplexes, in the presence of large amount of Gua, follow other preferential orientations than those

related to the strong interactions with the K^+ pattern on the mica surface.

The fact that lateral quadruplex-to-quadruplex interactions, even in the presence of external (opposing) forces, are effective to keep the hydrogel filaments aligned in a given direction paves the way for possible new biotech applications. An important example is related to the possibility to provide a supramolecular self-assembled hydrogel platform for the cultivation of cells in a three-dimensional oriented microenvironment^{24,25}. By controlling the Gua/GMP ratio, 3D cell cultures can grow with or without an anisotropic supporting scaffold, allowing for a misalignment or an alignment of the cells according to the template. This option can be of particular relevance in the case of use of the G-hydrogel as bioink for 3D bioprinting applications²⁶.

Author Contributions

Conceptualization: AP and PMa. Data curation: AP, PMo, FC and JSY. Formal Analysis: AP and PMa. Funding acquisition: RI and PMa. Investigation: AP, PMo, JSY and FC. Methodology: AP and PMa. Project administration: PMa. Software: AP. Supervision: RI and PMa. Visualization: AP and PMo. Writing (including review & editing) AP, RI and PMa.

Conflicts of interest

There are no conflicts to declare.

Acknowledgements

This research was partially funded by the European Union - Next Generation EU. Project Code: ECS00000041; Project Title: Innovation, digitalization and sustainability for the diffused economy in Central Italy - VITALITY. JSY acknowledges FAPESP (Brazil) for the Post-Doctoral fellowship process number 2018/07194-9. RI thanks to Conselho Nacional de Desenvolvimento Científico e Tecnológico (CNPq) for project number 401252/2014-0 and research fellowship.

References

- 1 S. Burge, G. N. Parkinson, P. Hazel, A. Todd and S. Neidle, *Nucleic Acids Research*, 2006, **34**, 5402–5415.
- 2 J. Sagi, *Journal of Biomolecular Structure and Dynamics*, 2014, **32**, 477–511.
- 3 xx, *Nucleic Acids Research*, 2015, **43**, 8627–8637.
- 4 H. Franz, F. Ciuchi, G. D. Nicola, M. D. Morais and P. Mariani, *Phys. Rev. E*, 1994, **50**, 395–402.

- 5 F. Federiconi, P. Ausili, G. Fragneto, C. Ferrero and P. Mariani, *J. Phys. Chem.*, 2005, **109**, 11037–11045.
- 6 P. Mariani, F. Spinozzi, F. Federiconi, H. Amenitsch, L. Spindler and I. Drevensek-Olenik, *J. Phys. Chem. B*, 2009, **113**, 7934–7944.
- 7 P. Mariani and L. Saturni, *Biophysical J.*, 1996, **70**, 2867–2874.
- 8 P. Mariani, F. Ciuchi and L. Saturni, *Biophysical J.*, 1998, **74**, 430–435.
- 9 F. Carducci, J. S. Yoneda, R. Itri and P. Mariani, *Soft Matter*, 2018, **14**, 2938–2948.
- 10 G. Nava, F. Carducci, R. Itri, J. S. Yoneda, T. Bellini and P. Mariani, *Soft Matter*, 2018, **15**, 2315.
- 11 M. Merino-Gómez, J. Gil, R. A. Perez and M. Godoy-Gallardo, *Int J. Mol. Sci.*, 2023, **24**, 4224.
- 12 L. Stefan and D. Monchaud, *Nat Rev Chem*, 2019, **3**, 650–668.
- 13 J. S. Yoneda, D. R. de Araujo, F. Sella, G. R. Liguori, T. T. A. Liguori, L. F. P. Moreira, F. Spinozzi, P. Mariani and R. Itri, *Materials Science and Engineering C*, 2021, **121**, 111834.
- 14 D. Necas and P. Klapetek, *Cent. Eur. J. Phys.*, 2012, **10**, 181–188.
- 15 <https://imagej.net/plugins/directionality>.
- 16 M. T. Sims, L. C. Abbott, R. M. Richardson, J. W. Goodby and J. N. Moore, *Liquid Crystals*, 2019, **46**, 11–24.
- 17 P. Davidson, D. Petermann and A. M. Levelut., *J Phys II*, 1995, 113–131.
- 18 P. G. de Gennes and J. Prost, *The Physics of Liquid Crystals*, Clarendon Press, Oxford, 1993.
- 19 T. T. Mills, G. E. S. Toombes, S. Tristram-Nagle, D.-M. Smilgies, G. W. Feigenson and J. F. Nagle, *Biophysical Journal*, 2008, **95**, 669–681.
- 20 J. Teixeira, *J. Appl. Cryst.*, 1988, **21**, 781–785.
- 21 R. V. Sharma and K. C. Sharma, *Physica*, 1977, **89A**, 213.
- 22 S. Nishimura, P. Biggs, T. Scales, W. Healy, K. Tsunematsu and T. Tateyama, *Langmuir*, 1994, **10**, 4554–4559.
- 23 K. Kunstelj, F. Federiconi, L. Spindler and I. Drevensek-Olenik, *Colloids and Surfaces B: Biointerfaces*, 2007, **59**, 120–127.
- 24 L. E. Buerkle, H. A. von Recum and S. J. Rowan, *Chem. Sci.*, 2012, **3**, 564–571.
- 25 A. Rotaru, G. Pricope, T. N. Plank, L. Clima, E. L. Ursu, M. Pintea, J. T. Davis and M. Barboiu, *Chem. Sci.*, 2012, **3**, 564–572.
- 26 A. Biswas, S. Malferrari, D. M. Kalaskar and A. K. Das, *Chem. Commun.*, 2018, **54**, 1778–1781.